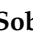



Article

Interplay of Ionic Species in Salts of Homoleptic Quaternary Phosphonium Cations Bearing Linear Biphenyl Moieties

Monica Bernard Tan ¹, Alexandre N. Sobolev ², Colin L. Raston ³ , Scott J. Dalgarno ^{4,*}  and Irene Ling ^{1,5,*}

¹ Centre for Fundamental and Frontier Sciences in Nanostructure Self-Assembly, Chemistry Department, Faculty of Science, University of Malaya, Kuala Lumpur 50603, Malaysia

² School of Molecular Sciences, M310, The University of Western Australia, Perth 6009, Australia

³ Flinders Institute for Nanoscale Science and Technology, College of Science and Engineering, Flinders University, Adelaide 5042, Australia

⁴ School of Engineering and Physical Sciences, Heriot-Watt University, Riccarton, Edinburgh EH14 4AS, UK

⁵ School of Science, Monash University Malaysia, Jalan Lagoon Selatan, Bandar Sunway 47500, Selangor, Malaysia

* Correspondence: s.j.dalgarno@hw.ac.uk (S.J.D.); ireneling@monash.edu (I.L.)

Abstract: Quaternary phosphonium salts are popular candidates used in many chemical transformations and synthetic chemistry, notably in catalysis. We have examined the single crystals of two bulky phosphonium compounds, tetra([1,1'-biphenyl]-4-yl) phosphonium dicyanamide ($C_{48}H_{36}P^+ \cdot N(CN)_2^-$, compound 1), and tetra([1,1'-biphenyl]-4-yl) phosphonium bromide hydrate ($C_{48}H_{36}P^+ \cdot Br^- \cdot CH_3CN \cdot H_2O$, compound 2), and herein report the structural properties for the compounds with an emphasis on the influence of the ion-ion interaction towards self-assembly; the overall self-assembly for both structures is very similar, with subtle differences in the cell parameters. The symmetrical tetra ([1,1'-biphenyl]-4-yl) phosphonium cations in both compounds self-assembled to form robust stacked columns in the solid-state, with voids occupied by anions or solvent molecules. Quantitative examination of intermolecular interactions using Hirshfeld surface analysis found that classical and non-classical hydrogen bonding appears to be the dominant contributor in stabilizing the self-assembly in both cases. The present work can not only benefit in understanding the mutual interaction between the sterically encumbered tetra ([1,1'-biphenyl]-4-yl) phosphonium cations and between counterions, but also provide insights for the self-assembled arrays in the solid-state.

Keywords: phosphonium; self-assembly; crystal structure; Hirshfeld surface; biphenyl



Citation: Tan, M.B.; Sobolev, A.N.; Raston, C.L.; Dalgarno, S.J.; Ling, I. Interplay of Ionic Species in Salts of Homoleptic Quaternary Phosphonium Cations Bearing Linear Biphenyl Moieties. *Crystals* **2023**, *13*, 59. <https://doi.org/10.3390/cryst13010059>

Academic Editor: Slawomir Grabowski

Received: 6 December 2022

Revised: 20 December 2022

Accepted: 21 December 2022

Published: 29 December 2022



Copyright: © 2022 by the authors. Licensee MDPI, Basel, Switzerland. This article is an open access article distributed under the terms and conditions of the Creative Commons Attribution (CC BY) license (<https://creativecommons.org/licenses/by/4.0/>).

1. Introduction

Phosphonium compounds are promising candidates for a myriad of applications due to their structural and stereochemical diversity and outstanding thermal and electrochemical stability and flexibility. The most commonly encountered phosphonium compounds have four organic substituents attached to a phosphorus center, forming the quaternary phosphonium cation. Along with a multitude of available anions, salts of these quaternary compounds are extensively used as Wittig reagents [1], phase transfer catalysts in asymmetric synthesis [2–6], ionic liquids [7–9], corrosion inhibitors [10], and polymer-based anion exchange membranes [11,12], as well as tracers for tumor imaging [13]. The versatility of the phosphonium quaternary compounds is known to be contributed by the different molecular features and self-organization of the ions within the compound. Hence, prior to designing functional organophosphorus materials, it is vital to understand the ubiquitous structure and the influence of governing intermolecular interactions on supramolecular self-assembly. Of particular interest, phosphonium compounds bearing at least two phenyl moieties can engage themselves in multiple phenyl embraces. These well-established aromatic interactions are strong and directional, and are capable of forming extended networks in the solid-state [14]. Dance et al. reported that for compounds containing tetraphenyl

phosphonium cations, the multiple phenyl embraces, namely the sixfold/sextuple and the fourfold/quadruple phenyl embrace, are found to be the dominant factor in the crystal supramolecularity [15–19]. Other commonly found intermolecular interactions are non-classical hydrogen bonding such as C-H \cdots X (X = O, N, F, Cl) and C-H \cdots π , which also play a significant role in crystal packing.

Over the years, we have judiciously studied the impact of a series of mono- and di-phosphonium salts towards the self-assembly of the ubiquitous *p*-sulfonatocalix[4]arene in a programmed manner [20]. These now well-established studies demonstrated that the use of large, bulky organophosphonium cations, and often in the presence of lanthanide(III) ions, was found to play a dominant role in driving the formation of different self-assembled supermolecules and packing arrangements. We note that the inclusion of the organophosphonium cations in the presence of *p*-sulfonatocalix[4]arene can be either (i) *endo*-cavity with the inclusion of one phenyl ring and/or (ii) *exo*-cavity with the phosphonium cations organized on the hydrophobic surface of the calixarene bilayers. An expansion to the calixarene bilayers was evident, where at the organic domain, the phosphonium molecules form a robust interlocking arrangement within themselves, and with calixarenes, through $\pi \cdots \pi$ interactions. Self-organization of the hydrophobic molecules within the hydrophobic surfaces of calixarenes results in the assembly of infinite chains, nets, or grid-like layers within the bilayers through the common multiple phenyl embrace, involving C-H \cdots π interactions and hydrogen bonding between the two components. Furthermore, we also reported unique crystal structures of various phosphonium salts which resulted from the metathetical ionic exchange between the phosphonium salts and N-heterocyclic compounds during the inclusion process in the presence of *p*-sulfonatocalix[4]arene [21,22].

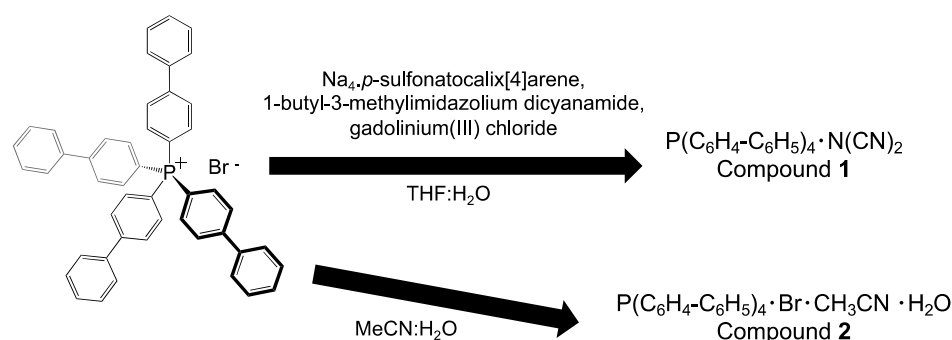
During our systematic investigations on the commonly reported tetraarylphosphonium salts, we noticed that the knowledge concerning bulkier phosphonium salts with polyaromatic rings is limited. We are focused on integrating geometrically complicated organophosphonium salts in self-assembled crystalline materials formed with *p*-sulfonatocalix[4]arene and a commercial available ionic liquid (1-butyl-3-methylimidazolium dicyanamide). Herein, we investigate the organization of a relatively new homoleptic quaternary aryl phosphonium compound containing symmetric biphenyl moieties (tetra-biphenyl phosphonium) linked in the 1,1' positions in which the aromatic rings create high steric hindrance directly around the cation charge associated with the phosphonium moiety. Understanding how the molecules pack in the solid-state is important as this would promote the design and fabrication of functional devices for targeted applications for which the current crystallographic details is sparse. Our anticipation of forming a new structural motif was hampered as the aggregation between the three components did not take place, but rather metathetical exchange between tetra-biphenyl phosphonium bromide with 1-butyl-3-methylimidazolium dicyanamide occurred. The X-ray crystallography analysis of two tetra-biphenyl phosphonium compounds bearing different anions are reported here, with the structural investigation augmented by Hirshfeld surface analysis with a view to understanding the characteristic intermolecular interactions, and to identify the dominant factors involved in directing their self-assembly behaviors. To-date, only one crystal structure pertaining to biphenyl substituents has been reported in the CCDC, however in that case the biphenyl moieties were attached to a larger silicon atom [23]. The analysis presented herein focuses on structural properties, in particularly self-assembly, an issue that is of general significance and that may be of interest to others working in this area.

2. Materials and Methods

All chemicals and solvents used were of analytical grade and obtained from commercial suppliers. These were used without further purification unless otherwise specified. Tetra-biphenyl phosphonium bromide salt was synthesized according to literature [24,25].

2.1. Synthesis

Three equivalents of gadolinium(III) chloride was added to an equimolar mixture of 1-butyl-3-methylimidazolium dicyanamide, tetra-biphenyl phosphonium bromide and sodium *p*-sulfonatocalix[4]arene in tetrahydrofuran and water (1:1). The solution was then warmed and slow evaporation at room temperature over several weeks afforded colourless plate-like crystals of $P(C_6H_4-C_6H_5)_4 \cdot N(CN)_2$, **1** (Scheme 1). Interestingly, **1** was formed as crystals by metathetical exchange involving tetra-biphenyl phosphonium bromide with 1-butyl-3-methylimidazolium dicyanamide in the presence of sodium *p*-sulfonatocalix[4]arene and lanthanide, though the latter is not included in the resulting crystalline material. Prism-shaped crystals of **2** were formed on slow evaporation of tetra-biphenyl phosphonium bromide salt in a 1:1 mixture of acetonitrile and water (Scheme 1).



Scheme 1. Synthesis of **1** and **2**.

2.2. Single Crystal X-ray Crystallography

All data were measured from multiple crystals to ensure the homogeneity of the materials using an Oxford Xcalibur-S (**1**) and Oxford Gemini-R Ultra (**2**) CCD diffractometers at 100(2) K with monochromatic $MoK\alpha$ ($\lambda = 0.71073 \text{ \AA}$) and $CuK\alpha$ ($\lambda = 1.54178 \text{ \AA}$) radiation, respectively. Data were corrected for Lorentz and polarization effects, and absorption correction applied using multiple symmetry equivalent reflections. The structures were solved by direct methods and refined against F^2 with full-matrix least-squares using the program suite SHELX [26]. Anisotropic displacement parameters were employed for the non-hydrogen atoms. One of the N-atoms in **1** is disordered. All hydrogen atoms were added at calculated positions and refined using a riding model with isotropic displacement parameters based on those of the parent atom. Crystallographic data for the structures reported in this paper have been deposited at the Cambridge Crystallographic Data Centre. Copies of data with CCDC numbers 2211649–2211650 can be obtained free of charge via <https://www.ccdc.cam.ac.uk/structures/> (accessed on 6 December 2022), or from the Cambridge Crystallographic Data Centre, 12 Union Road, Cambridge CB2 1EZ, UK (Fax: +441223336033; email: deposit@ccdc.cam.ac.uk). The Hirshfeld surfaces, 2D fingerprint plots and the energy framework analysis were generated using CrystalExplorer17 [27]. It is important to note that C-H bond distance is set as 1.083 \AA whilst that for O-H is set as 0.983 \AA in CrystalExplorer.

3. Results

The two crystalline tetra-biphenyl phosphonium salts, **1** and **2**, have $N(CN)_2^-$ and Br^- anions, respectively), and have not previously been structurally authenticated. This was undertaken herein with an aim to understand the nature of the interactions between the cations and between the anions, and the cation–anion interplay in balancing electrostatic attraction and repulsion. Both solid-state structures exhibit the same structural motif, having very similar cell parameters, crystallizing in a triclinic system, and have been solved in the $P\bar{1}$ space group. The asymmetric unit found in the structure of **1** comprises one tetra-biphenyl phosphonium cation and a disordered dicyanamide anion, whilst that in **2** contains one tetra-biphenyl phosphonium cation, a bromide anion, and an acetonitrile

and water of crystallization. Full crystallographic data and details for these structures are summarized in Table S1.

3.1. Structural Description

3.1.1. Molecular Features of Tetra-Biphenyl Phosphonium Cation

The molecular structure of the tetra-biphenyl phosphonium cation in **1** is shown in Figure 1a. Owing to the presence of a different counterions, the tetra-biphenyl phosphonium cation in **2** has subtle structural differences in terms of the bond angles and lengths when compared with those found in **1**. The tetrahedral symmetry of the central phosphorus atom in both compounds is slightly distorted, which is evident from the varying C-P-C bond angles, as tabulated in Table S2. The interplanar angles between the inner and outer aromatic rings, as shown in Figure 1b, differ for all four biphenyl units with their angles listed in Table S2. Interestingly, the interplanar angle at ring 3a/ring 3b in **2** is significantly larger than in **1**, indicating a more twisted biphenyl unit. This feature has led to an additional intermolecular interaction observed in **2**, details of which are presented in the discussion section. All reported interplanar angles are greater than the ideal interplanar angle of 0° observed in a stable, isolated biphenyl in its crystalline state [28]. In general, the differences in molecular features of the cations observed are due to steric necessities for close packing and electrostatic interaction between the ions.

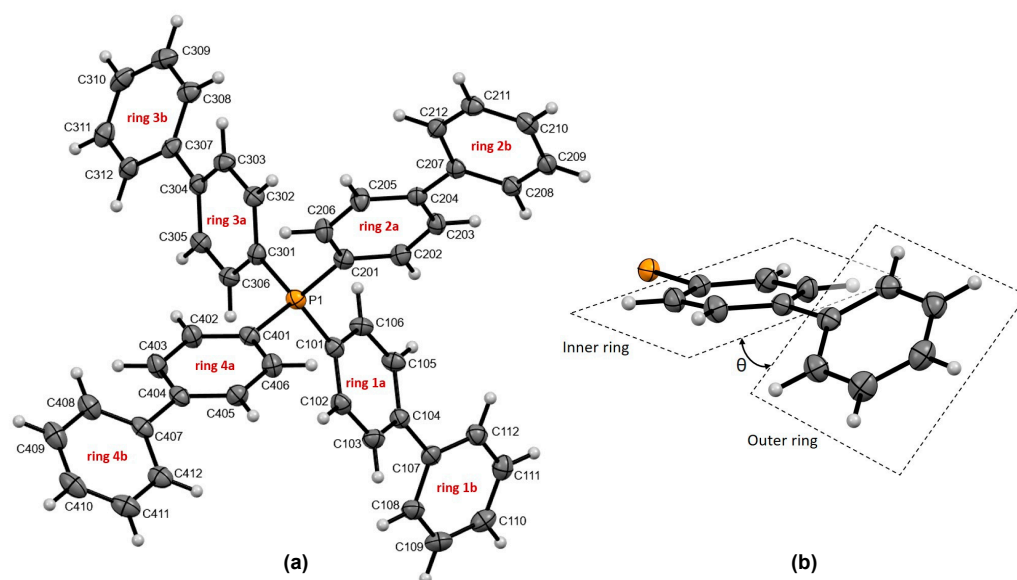


Figure 1. (a) ORTEP [29] view of the molecular structure of tetra-biphenyl phosphonium cation for **1**. Ellipsoids are drawn at 50% probability level. Salt **2** has similar cation structure and follows the same numbering scheme as in **1**. (b) The interplanar angle between inner and outer (closer to or further from the phosphorus centre, respectively) aromatic ring of a single biphenyl unit.

3.1.2. Self-Assembly

Examination of the extended structures shows that the phosphonium cations in both crystal structures exhibit similar self-assembly behavior, as shown in Figure 2. Two phosphonium cations are arranged in opposite orientations, forming a phosphonium pair (one purple and one orange molecule) with closest P...P distances of 7.91 Å and 8.05 Å for **1** and **2**, respectively. The packing in both crystals consists of phosphonium pairs propagated by translational operations, resulting in parallel horizontal columns, as viewed down the *a*-axis, that are devoid of the common phenyl embrace interactions. From another point of view, inspection of packing through the crystallographic *c*-axis reveals that cations form stacked columns with voids occupied by $N(CN)_2^-$ in **1**, and Br^- , CH_3CN and H_2O in **2**. The occurrence of similar cationic packing in the presence of differing anions and

additional solvent of crystallization suggests that this assembly mode may be more stable than other alternatives.

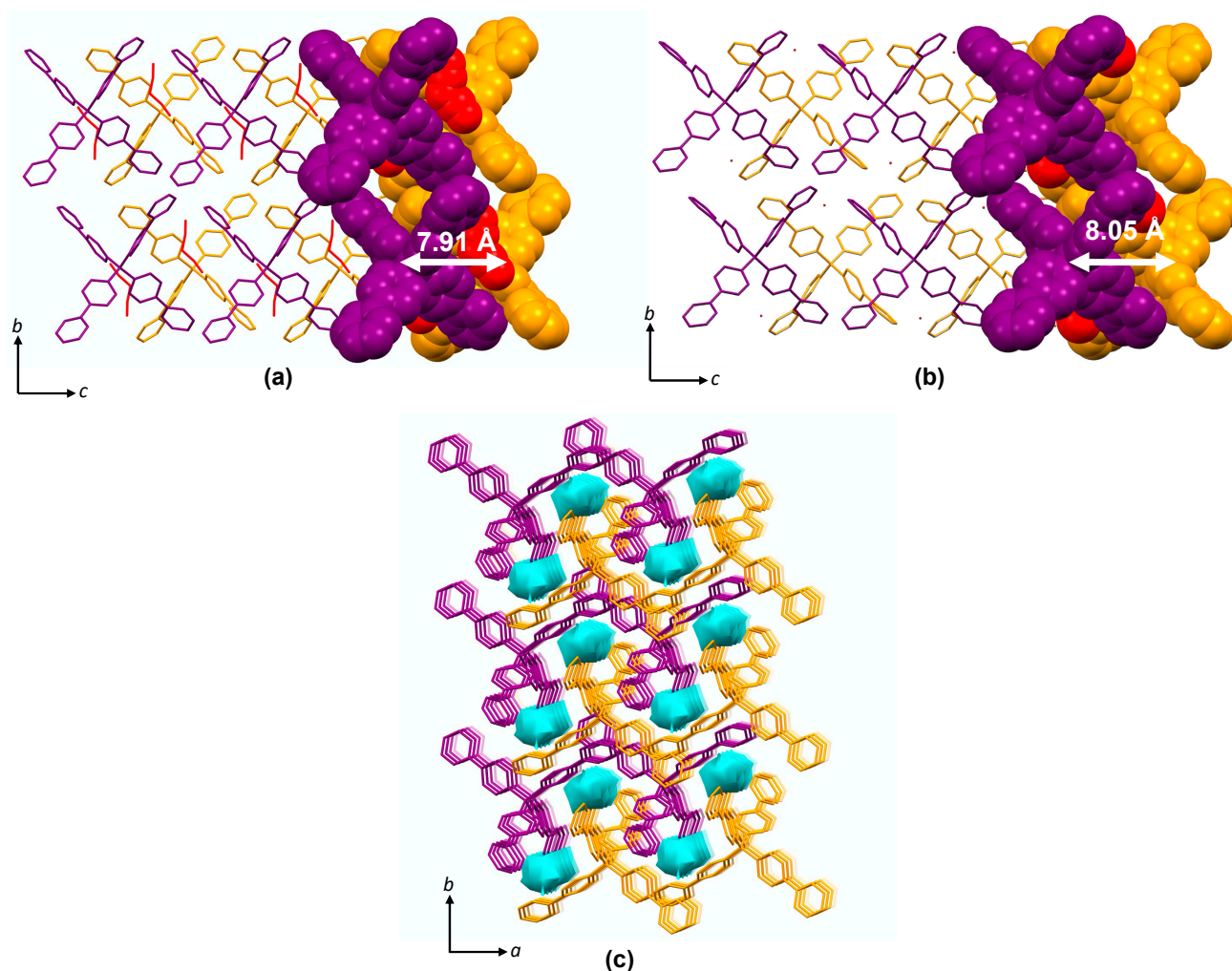


Figure 2. Partial space filling representation depicting the self-assembly of **1** (a) and **2** (b) viewed down the crystallographic *a*-axis. A phosphonium cation pair is highlighted as one purple and one orange species in each case, with closest P...P distances of 7.91 Å and 8.05 Å for **1** and **2**, respectively. Anions are highlighted in red space filling representations. Light blue surfaces represent the voids occupied by $\text{N}(\text{CN})_2^-$ anions in **1**, or Br^- anions and solvent molecules in **2**. (c) Visualization of the calculated void volume within the crystal lattice of **1** is 45.4%. Similar packing arrangement with voids within the crystal lattice is found for **2** with a calculated void volume of 54.5%. Hydrogen atoms and solvent molecules are omitted for clarity.

Packing involving C–H... π interactions is commonly observed in supramolecular assemblies. Two significant C–H... π interactions are observed in **1**: C(106)–H(106)... π (ring 2b) and C(211)–H(211)... π (ring 3b) with respective distances of 2.68 Å and 2.79 Å (Figure 3a). Similar respective interactions are also found in **2** with slightly longer distances of 2.90 Å and 2.84 Å relative to those found in **1**. The structure of **2** displays an additional C–H... π interaction at C(206)–H(206)... π (ring 3b) with a distance of 2.69 Å which relates to the more twisted conformation on its aromatic ring 3a/ring 3b (with interplanar angle of 35.2° compared to 27.4° in **1**, Figure 3b). There are no obvious π ... π interactions observed in both crystals, with the shortest centroid to centroid distance between parallel aromatic rings within and between phosphonium pairs is more than 4 Å [30].

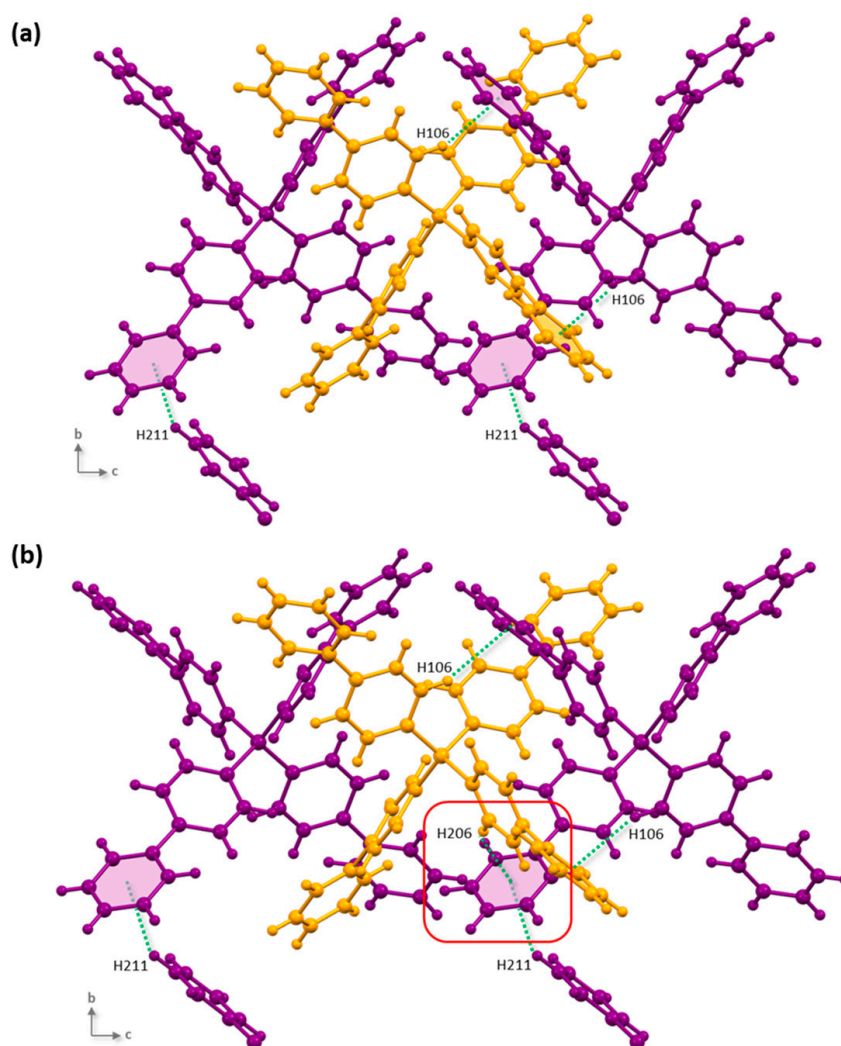


Figure 3. Ball-and-stick representation of C–H \cdots π interactions between phosphonium cations in **1** (a) and **2** (b), with the red square highlighting an additional crystallographically unique C–H \cdots π interaction found in **2**.

The anions and solvent molecules fit in the voids formed by the packing of phosphonium cations (Figure 2c); the volume of the voids in **1** and **2** were calculated as 45.38% and 54.53%, respectively using a solvent probe of 0.9 Å and a grid spacing of 1.2 Å. In **1** the $\text{N}(\text{CN})_2^-$ anion participates in multiple C–H \cdots N interactions with calculated close contacts of 2.64 Å, 2.63 Å and 2.62 Å for C(102)–H(102) \cdots N(0) (symmetry: $-x + 1, -y + 1, -z + 1$), C(312)–H(312) \cdots N(1) (symmetry: $x - 1, y, z$), and C(203)–H(203) \cdots N(2), respectively (Figure 4a). The $\text{N}(\text{CN})_2^-$ anion also exhibits close C \cdots H contacts (C-atoms from the cyano-group to the phosphonium phenyl H-atoms) with distances of 2.86 Å to 2.94 Å. The bond lengths in $\text{N}(\text{CN})_2^-$ are within the expected range with N–C distances ranging from 1.132 (4) Å to 1.335 (3) Å. In **2**, there are multiple hydrogen bonding interactions present between anion, cation and solvent molecules, as illustrated in Figure 4b. The Br^- ion displays relatively strong H \cdots Br interactions with H-atoms from the water and acetonitrile of crystallization, with respective distances of 2.55 Å and 2.77 Å. The Br^- interaction with phenyl H-atoms at H(412) (2.81 Å) and H(312) (2.85 Å) are longer and presumably weaker than the aforementioned H \cdots Br interaction. Other hydrogen bonds present in the crystal structure include a C–H \cdots N interaction at 2.85 Å and C–H \cdots O interactions with distances at 2.58 Å and 2.62 Å.

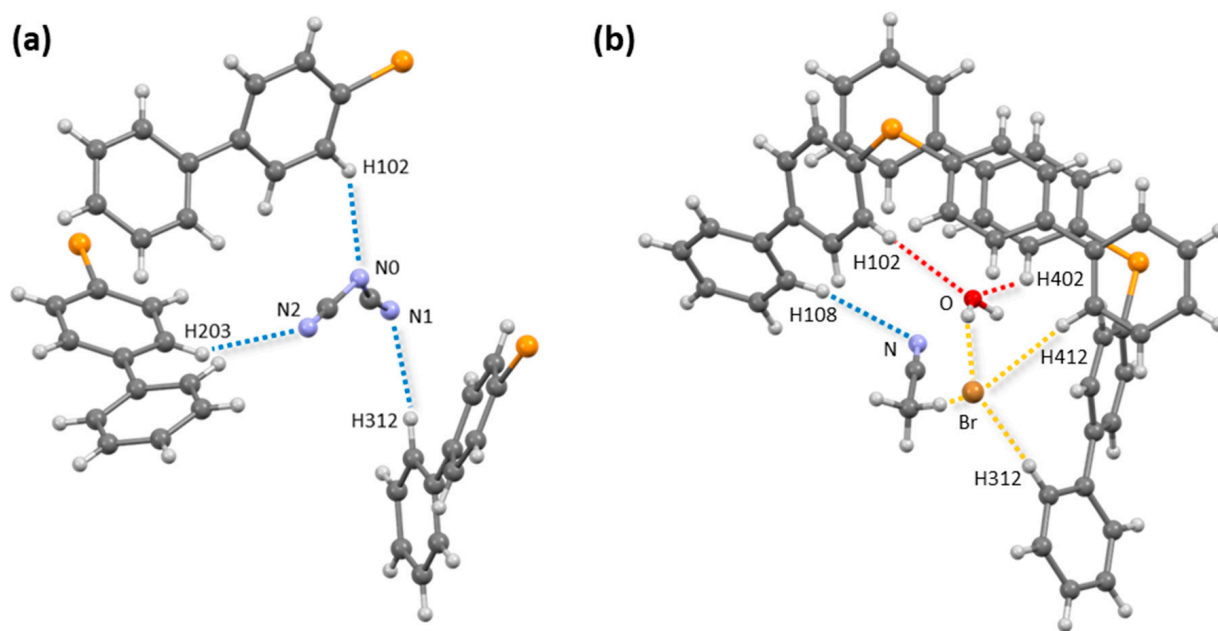


Figure 4. Ball-and-stick representation of intermolecular interactions involving $\text{N}(\text{CN})_2^-$ in compound **1** (a) and CH_3CN , H_2O , and Br^- in compound **2** (b). $\text{C-H}\cdots\text{N}$, $\text{C-H}\cdots\text{O}$ and $\text{C-H}\cdots\text{Br}$ close contacts are represented by blue, red and yellow lines, respectively.

3.1.3. Hirshfeld Surface Analysis

Interactions in both crystals can be further described with the aid of two-dimensional fingerprint plots generated from the Hirshfeld surface analyses using CrystalExplorer17 [27], which provides information on the relative contribution of various intermolecular interactions present in the crystal structure. Figure 5a,b depicts the fingerprint plot of cation and anion in **1** and **2**, respectively. The relative contributions of various intermolecular interactions, in terms of percentages, to the cation Hirshfeld surface are summarized in the pie-charts displayed below the fingerprint plots. It is observed that intermolecular $\text{H}\cdots\text{H}$ bonding appears to be the primary contributor in the crystal packing of both compounds (45.8% in **1** and 50.4% in **2**), which is consistent with the high proportion of hydrogen atoms present in the crystal structure. The second major contributor is attributed to reciprocal $\text{C}\cdots\text{H}/\text{H}\cdots\text{C}$ contact encompassing 40.0% in **1** and 38.8% in **2**. In **1**, interactions of $\text{H}\cdots\text{N}$ (9.6%) and $\text{C}\cdots\text{C}$ (4.1%) are found at a slightly higher percentage compared to **2**, and $\text{C}\cdots\text{N}$ interactions with the lowest contribution of 0.5% completes the Hirshfeld surface. Additional charge assisted non-classical hydrogen bonds of $\text{H}\cdots\text{Br}$, $\text{H}\cdots\text{O}$ and $\text{C}\cdots\text{O}$ contribute 2.7%, 1.2% and 0.5%, respectively, making up the residual Hirshfeld surface for **2**. In the anion fingerprint plot, the green region towards the spikes and some red streaking represents greater relative contribution of hydrogen bonding on the surface. The $\text{C-H}\cdots\text{N}$ interaction (64.4%) is the major contributor in the $\text{N}(\text{CN})_2^-$ surface in **1**, whilst for **2** the $\text{Br}\cdots\text{H-C}$ interaction (99.9%) dominates the anion Hirshfeld surface. Salt **2** has less efficient close packing compared to **1** as evidenced by the extended contact distances at higher d_e and d_i value, as well as a larger percentage of void volume. Energy framework analysis (generated from CrystalExplorer17) was also used to visualize the interaction topology within the crystal structures. The prevailing intermolecular interaction energies in the crystal structures are denoted as thick cylinders joining the molecules. From the analysis, it is not surprising that the dispersion contribution dominates the intermolecular interactions for both structures. The zigzag tubes intersect the molecular sheets along the a - and b -axes in **1**, Figure 6. Similar energy distribution patterns were found for **2**.

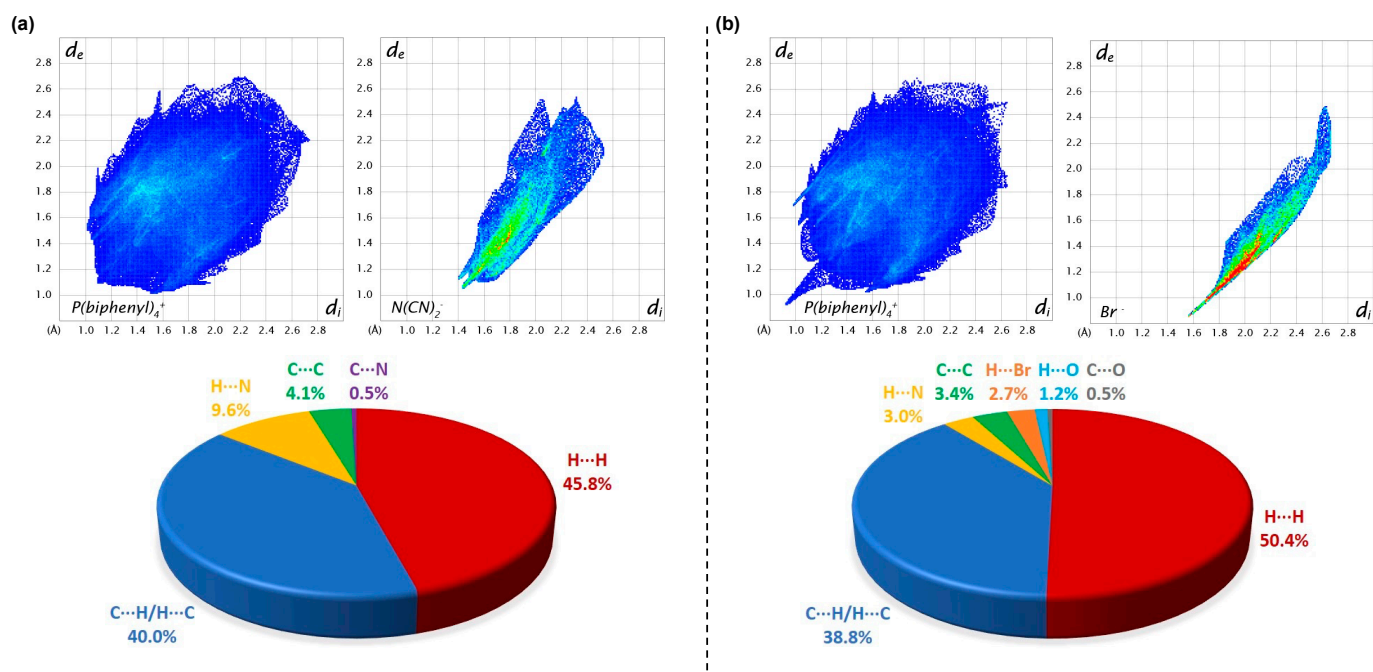


Figure 5. Fingerprint plots of tetra-biphenyl phosphonium cation and counterions $(N(CN)_2)^-$ and Br^- for compounds **1** (a) and **2** (b), in addition to relative contributions of the intermolecular contacts (in percentages) to the Hirshfeld surfaces.

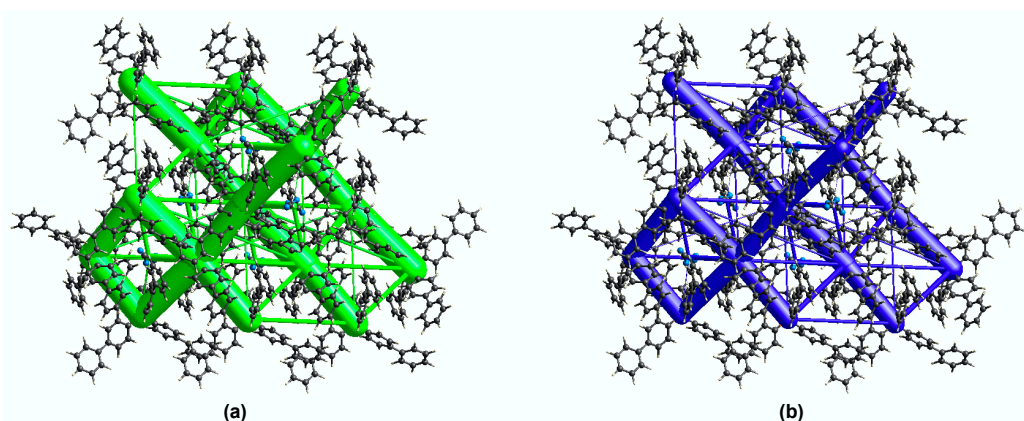


Figure 6. Energy frameworks for **1**, representing (a) the dispersion energy (green colour) and (b) the net interaction energy (in blue colour).

4. Discussion

The Cambridge Structural Database (CSD, Version 5.42, updated September 2021) was searched for tetra([1,1'-biphenyl]-4-yl) phosphonium salts. There were no comparable structures found for such species. The best structural comparison to **1** and **2** is provided by CCDC refcode ZZZUJT [23], which differs structurally in terms of the overall packing in that the bulky tetraphenylsilane crystallized in the tetragonal space group $I\bar{4}$. The interplanar angle for all the biphenyl moieties is 31.55° , and this is within the range of the measured interplanar angles found in the structures of **1** and **2**.

We have demonstrated the self-aggregation of the tetra-biphenyl phosphonium molecules into a stacked-column is robust with the smaller counterions and solvent molecules filling interstitial channels/voids. It is noteworthy that the presence of the different types of counterions and/or solvent molecules does not significantly influence the structural motifs of the bulky phosphonium cations, except for the subtle close P...P distances. Crystal-Explorer has in turn enabled us to rationalize the multifaceted classical and non-classical

hydrogen-bonding patterns in the tetra-biphenyl phosphonium salts which contributed to the very similar structural motifs between the two reported structures.

5. Conclusions

In conclusion, the crystal structures of tetra-biphenyl phosphonium salts with either $\text{N}(\text{CN})_2^-$ (1) or Br^- (2) anions are reported. Single crystal X-ray diffraction analysis revealed that both compounds crystallize in the same triclinic system, with structure solution being performed for both cases in the space group $P\bar{1}$. The molecular features of the phosphonium cation in 1 and 2 have subtle differences, of particular interest being the larger interplanar angles displayed in 2 which results in an additional $\text{C-H}\cdots\pi$ interaction being observed in the extended structure. The salts exhibit analogous packing behavior in which the phosphonium cations assemble in stacked columns with voids occupied by anions and solvent molecules. Although it is common for phenyl containing compounds to form embraces, from the results presented herein it is seen that tetra-biphenyl phosphonium does not exhibit such interactions, but rather it is held together by multiple non-classical hydrogen bonding. Hirshfeld surface analyses revealed that intermolecular $\text{H}\cdots\text{H}$ interactions appear to be the dominant contributor in stabilizing the phosphonium cation self-assembly in both compounds, followed by $\text{C-H}\cdots\pi$ interactions.

Supplementary Materials: The following supporting information can be downloaded at: <https://www.mdpi.com/article/10.3390/cryst13010059/s1>, Table S1: Crystallographic data and refinement parameters; Table S2: Relevant geometrical parameters; Table S3: Selected hydrogen-bond geometry (\AA , $^\circ$) for Compound 2.

Author Contributions: Conceptualization, I.L.; methodology, I.L.; software, M.B.T. and I.L.; validation, A.N.S. and I.L.; formal analysis, M.B.T. and I.L.; data curation, M.B.T., A.N.S. and I.L.; writing—original draft preparation, M.B.T. and I.L.; writing—review and editing, A.N.S., I.L., S.J.D. and C.L.R.; visualization, I.L., A.N.S. and S.J.D.; project administration, I.L.; funding acquisition, I.L. and C.L.R. All authors have read and agreed to the published version of the manuscript.

Funding: We thank the Ministry of Higher Education Malaysia for financial support from the Fundamental Research Grant Scheme (FRGS/1/2018/STG01/UM/02/4). This research was also funded by the Australian Research Council (ARC) and the University of Western Australia.

Data Availability Statement: Crystal structures of 1 and 2 have been deposited in the CCDC database (2211649 and 2211650).

Conflicts of Interest: The authors declare no conflict of interest.

References

1. Wang, M.-L.; Liu, B.-L.; Lin, S.-J. Synthesis of an active quaternary phosphonium salt and its application to the Wittig reaction: Kinetic study. *J. Chin. Inst. Chem. Eng.* **2007**, *38*, 451–459. [[CrossRef](#)]
2. Noroozi-Shad, N.; Gholizadeh, M.; Sabet-Sarvestani, H. Quaternary phosphonium salts in the synthetic chemistry: Recent progress, development, and future perspectives. *J. Mol. Struct.* **2022**, *1257*, 132628. [[CrossRef](#)]
3. Liu, S.; Kumatabara, Y.; Shirakawa, S. Chiral quaternary phosphonium salts as phase-transfer catalysts for environmentally benign asymmetric transformations. *Green Chem.* **2016**, *18*, 331–341. [[CrossRef](#)]
4. Enders, D.; Nguyen, T. Chiral quaternary phosphonium salts, a new class of organocatalysts. *Org. Biomol. Chem.* **2012**, *10*, 5327–5331. [[CrossRef](#)] [[PubMed](#)]
5. He, R.; Wang, X.; Hashimoto, T.; Maruoka, K. Binaphthyl-Modified Quaternary Phosphonium Salts as Chiral Phase-Transfer Catalysts, Asymmetric Amination of β -Keto Esters. *Angew. Chem. Int. Ed.* **2008**, *47*, 9466–9468. [[CrossRef](#)]
6. Manabe, K. Asymmetric phase-transfer alkylation catalyzed by a chiral quaternary phosphonium salt with a multiple hydrogen-bonding site. *Tetrahedron Lett.* **1998**, *39*, 5807–5810. [[CrossRef](#)]
7. Castillo, J.; Teresa, M.; Fortuny, A.; Navarro, P.; Sepúlveda, R.; María, A. Cu(II) extraction using quaternary ammonium and quaternary phosphonium based ionic liquid. *Hydrometallurgy* **2014**, *141*, 89–96. [[CrossRef](#)]
8. Fraser, K.J.; MacFarlane, D. Phosphonium-Based Ionic Liquids, An Overview. *Aust. J. Chem.* **2009**, *62*, 309–321. [[CrossRef](#)]
9. Del Sesto, R.E.; Corley, C.; Robertson, A.; Wilkes, J.S. Tetraalkylphosphonium-based ionic liquids. *J. Organomet. Chem.* **2005**, *690*, 2536–2542. [[CrossRef](#)]
10. Nahlé, A.H.; Harvey, T.; Walsh, F. Quaternary aryl phosphonium salts as corrosion inhibitors for iron in HCl. *J. Alloys Compd.* **2018**, *765*, 812–825. [[CrossRef](#)]

11. Wang, C.; Tao, Z.; Zhao, X.; Li, J.; Ren, Q. Poly(aryl ether nitrile)s containing flexible side-chain-type quaternary phosphonium cations as anion exchange membranes. *Sci. China Mater.* **2020**, *63*, 533–543. [[CrossRef](#)]
12. Gu, S.; Cai, R.; Luo, T.; Jensen, K.; Contreras, C.; Yan, Y. Quaternary Phosphonium-Based Polymers as Hydroxide Exchange Membranes. *ChemSusChem* **2010**, *3*, 555–558. [[CrossRef](#)] [[PubMed](#)]
13. Min, J.-J.; Biswal, S.; Deroose, C.; Gambhir, S.S. Tetraphenylphosphonium as a Novel Molecular Probe for Imaging Tumors. *J. Nucl. Med.* **2004**, *45*, 636–643. [[PubMed](#)]
14. Dance, I.; Scudder, M. Molecules embracing in crystals. *CrystEngComm* **2009**, *11*, 2233–2247. [[CrossRef](#)]
15. Dance, I.; Scudder, M. Supramolecular Motifs: Concerted Multiple Phenyl Embraces between Ph_4P^+ Cations Are Attractive and Ubiquitous. *Chem.-Eur. J.* **1996**, *2*, 481–486. [[CrossRef](#)]
16. Dance, I.; Scudder, M. Concerted supramolecular motifs: Linear columns and zigzag chains of multiple phenyl embraces involving Ph_4P^+ cations in crystals. *J. Chem. Soc. Dalton Trans.* **1996**, *19*, 3755–3769. [[CrossRef](#)]
17. Scudder, M.; Dance, I. Crystal supramolecular motifs. Two- and three-dimensional networks of Ph_4P^+ cations engaged in sixfold phenyl embraces. *J. Chem. Soc. Dalton Trans.* **1998**, *19*, 3167–3176. [[CrossRef](#)]
18. Scudder, M.; Dance, I. Crystal supramolecular motifs. Ladders, layers and labyrinths of Ph_4P^+ cations engaged in fourfold phenyl embraces. *J. Chem. Soc. Dalton Trans.* **1998**, *19*, 3155–3166. [[CrossRef](#)]
19. Scudder, M.; Dance, I. Sixfold phenyl embraces with substituted phenyl in PPh_3 . *J. Chem. Soc. Dalton Trans.* **2000**, *17*, 2909–2915. [[CrossRef](#)]
20. Ling, I.; Raston, C.L. Sulfonato and Phosphonatocalix[n]arenes in Self-Assembly. In *Comprehensive Supramolecular Chemistry II*; Atwood, J.L., Gokel, G.W., Barbour, L.J., Eds.; Elsevier: Amsterdam, The Netherlands, 2017; Volume 6, pp. 19–73.
21. Ling, I.; Skelton, B.W.; Sobolev, A.N.; Alias, Y.; Khor, Z.C.; Raston, C.L. Effect of anions on the solid-state interplay of symmetric and unsymmetric phosphonium cations. *New J. Chem.* **2020**, *44*, 10220–10228. [[CrossRef](#)]
22. Ling, I.; Alias, Y.; Sobolev, A.N.; Raston, C.L. Hirshfeld surface analysis of phosphonium salts. *CrystEngComm* **2010**, *12*, 4321–4327. [[CrossRef](#)]
23. Schwarzer, A.; Schilling, I.C.; Seichter, W.; Weber, E. Synthesis and X-ray Crystal Structures of New Tetrahedral Arylethynyl Substituted Silanes. *Silicon* **2009**, *1*, 3–12. [[CrossRef](#)]
24. Budzelaar, P.H.M.; Van Doorn, J.A.; Meijboom, N. Reductive cleavage of the carbon-phosphorus bond with alkali metals. I. Cleavage of functionalised triphenylphosphines; formation of secondary and primary phosphines. *Recl. Trav. Chim. Pays-Bas* **1991**, *110*, 420–432. [[CrossRef](#)]
25. Worrall, D.E. Studies in The Diphenyl Series. III. Some Phosphorus Derivatives of Diphenyl. *J. Am. Chem. Soc.* **1930**, *52*, 2933–2937. [[CrossRef](#)]
26. Sheldrick, G.M. Crystal Structure Refinement with SHELXL. *Acta Cryst.* **2015**, *C71*, 3–8.
27. Spackman, P.R.; Turner, M.J.; McKinnon, J.J.; Wolff, S.K.; Grimwood, D.J.; Jayatilaka, D.; Spackman, M.A. CrystalExplorer: A program for Hirshfeld surface analysis, visualization and quantitative analysis of molecular crystals. *J. Appl. Cryst.* **2021**, *54*, 1006–1011. [[CrossRef](#)]
28. Casalone, G.; Mariani, C.; Mugnoli, A.; Simonetta, M. The molecular structure of biphenyl in the gas and solid phases. *Mol. Phys.* **1968**, *15*, 339–348. [[CrossRef](#)]
29. Johnson, C.K. *ORTEP II. Report ORNL-5138*; Oak Ridge National Laboratory: Oak Ridge, TN, USA, 1976.
30. Nishio, M. CH/π hydrogen bonds in crystals. *CrystEngComm* **2004**, *6*, 130–158. [[CrossRef](#)]

Disclaimer/Publisher’s Note: The statements, opinions and data contained in all publications are solely those of the individual author(s) and contributor(s) and not of MDPI and/or the editor(s). MDPI and/or the editor(s) disclaim responsibility for any injury to people or property resulting from any ideas, methods, instructions or products referred to in the content.